Available online at www.sciencedirect.com

ScienceDirect

Procedia CIRP 94 (2020) 731–736

www.elsevier.com/locate/procedia

11th CIRP Conference on Photonic Technologies [LANE 2020] on September 7-10, 2020

Simulation of keyhole laser welding of stainless steel plates with a gap

Pierre Drobniak[a], Andreas Otto[a], Rodrigo Gómez Vázquez[a], Rosa Maria Arias[b], Jorge Luis Arias[b,*]

[a]*Vienna University of Technology, Faculty of Mechanical and Industrial Engineering, Karlsplatz 13, 1040 Vienna, Austria*
[b]*AIMEN, Polígono Industrial de Cataboi SUR-PPI-2 (Sector) 2, Parcela 3, E36418 – O Porriño – Pontevedra, Spain*

* Corresponding author. Tel.: +43-158-801-311-624; *E-mail address:* pierre.drobniak@tuwien.ac.at

Abstract

The presence of a gap (from tens to hundreds of microns) between two components may cause defects during laser-welding processes. Within this paper the process is investigated for two stainless steel plates in overlap configuration by means of multiphysyical CFD modeling. As a first step modeling results are compared with experimental data. Then the gap influence on the fluid dynamics and on the appearance of welding defects are analyzed. Based on the results adapted beam shapes are proposed that allow for an optimized energy distribution and thus an improved weld quality.

Keywords: laser welding with gap; VoF-modelling; keyhole; meltpool dynamics; process optimisation

1. Introduction

Laser welding processes are already widely used in industry. Hence their study is of great interest. However, real time experimental investigations, for instance through high speed cameras, are often impractical and results interpretation remains tricky. One could also proceed to post-experimental analysis, but this method usually is invasive and does not yield enough information on process dynamics. In this context, 3D-simulation is an interesting tool, providing exclusive real-time information on physical mechanisms involved [1].

Most of laser welding processes in overlap configuration are intended to be carried out with two plates in contact. However, this contact sometimes induces blowholes, spatter and lack of fusion [2] especially when welding zinc coated steel sheets. For this reason, some welding processes (in automotive industry for instance) involve a gap within a range from 50-100 microns up to a few 100 microns [2]. However, the presence of a gap also induces defects, such as porosity or underfill [3]. A better understanding of physical mechanisms leading to gap-induced defects seems of particular importance. Moreover, a way to counterbalance the appearance of these welding imperfections would enable an improvement of industrial processes.

The following paper will shed light on those interrogations and provide adapted beam shapes solutions for several gap values. In this context, the study will first introduce the multi-physical model used, then validate it by comparing simulations results with experimental data. Thereafter, the gap influence on fluid dynamics and on the appearance of welding defects will be investigated. Based on these results, adapted beam shapes that allow for an optimized energy distribution and thus an improved weld quality are proposed.

10.1016/j.procir.2020.09.134

Nomenclature

ρ	density (kg/m³)
M	molar mass (kg/mol)
T	melting temperature (K)
T	boiling temperature (K)
C	heat capacity (J/K)
C	heat capacity (J/K)
λ	thermal conductivity (W/m/K)
σ	surface energy (J/m²)
n	refractive index
κ	extinction coefficient
P	laser power (kW)
M²	laser beam quality factor
W_0	laser beam waist at focus (µm)
W	laser beam waist at the material surface ()
V	laser scanning speed (mm/s)
γ	initial laser scanning acceleration (m/s²)
D	laser defocus (mm)
G	gap between plates (µm)
a	ellipse semi-major axis (µm)
b	ellipse semi-minor axis (µm)

2. Model presentation

2.1. Program presentation

The software package used for the simulations within this research work has been developed at TU Vienna on top of the OpenFOAM® environment and is based on the Volume of Fluids discretization method. Navier-Stokes equations are solved by means of a PIMPLE-algorithm loop.

This simulation software allows for the combination of multi physical phenomena, among which are: laser propagation, fluid dynamics, heat transfer, phase change of a multi-phase mixture (in our case solid, liquid and vapor), optical propagation, surface tension. More information on the software can be found in [4, 5, 6].

2.2. Simulation parameters

Table 1. Simulation material parameters.

	Solid	Liquid	Vapour
ρ	7.85x10³ (300K) 7.2x10³ (1710K)	6.9x10³ (1700K) 5.5x10³ (3500K)	Ideal gas model
M	55.8 x10^{-3}	55.8 x10^{-3}	55.8 x10^{-3}
T_m	1700	-	-
T_b	-	3134	-
C	483 (300K) 684 (1700K)	800	477 (3134K) 714 (6000K)
λ	15 (300K) 36 (1800K)	27 (1800K) 42 (3000K)	0.10 (1900K) 0.25 (10000K)
σ	0.5 (300K) 1.5 (1000K) 1.88 (1700K)	1.88 (1700K) 1.3 (3300K)	0
(n,κ)	(3.80; 5.00)	(3.80; 5.00)	(1; 0)

The material chosen is AISI304L stainless steel. The atmosphere is assumed to be air. Table 1 gives information on the simulation material parameters. When a value is given for different temperatures, all intermediate values are linearly interpolated. All values outside of the temperature boundaries are equal to the boundary value.

The laser wavelength is 1070 µm. Initial temperatures for air and material are both 298.15K.

Each plate has the following dimensions: 20 x 4 x 1 mm. Fig. 1 presents an overview of the configuration.

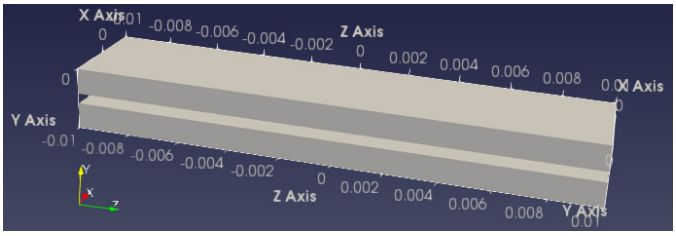

Fig. 1. Simulation overview (0.4mm gap in this example)

The laser track starts at -8mm and finishes at +8mm. The laser head starts from a rest position (V = 0) with a constant acceleration γ until it reaches its cruising speed V.

Four configurations are investigated (see Table 2).

Table 2. List of simulations.

Name	G (µm)	V (mm/s)	γ (m/s²)	P (kW)	M²	D (mm)	W_0 (µm)	W (µm)
S1	100	100	3	4.00	8	+4.83	60.5	226
S2	200	100	3	4.00	8	+4.83	60.5	226
S3	300	100	3	4.00	8	+4.83	60.5	226
S4	400	100	3	4.00	8	+4.83	60.5	226

3. Model validation

3.1. Experimental parameters

Four experiments are carried out: E1, E2, E3 and E4. They respectively correspond to simulations S1, S2, S3 and S4. The laser beam radii at focus and material surface are W_0 = 60.5 µm and W = 291 µm respectively.

A parameter missing from the experiment is the initial acceleration. Its value is assessed to be 3 m/s².

In the experiments, care was taken to avoid any edge effects (at least 5mm away from the edges).

After each experiment a cross-section is taken around 7 cm away from the starting position and a longitudinal section is taken, from the starting point to approximately 3 cm.

3.2. Comparison between experiments and simulations

Fig. 2, Fig. 3, Fig. 4 and Fig. 5 respectively show a comparison between E1, E2, E3, E4 and S1, S2, S3, S4. A vertical white line in the longitudinal section shows where the cross-section was taken from the simulation. A red contour indicates the liquid-solid boundary.

Artwork has no text along the side of it in the main body of the text. However, if two images fit next to each other, these may be placed next to each other to save space. For example, see Fig. 1.

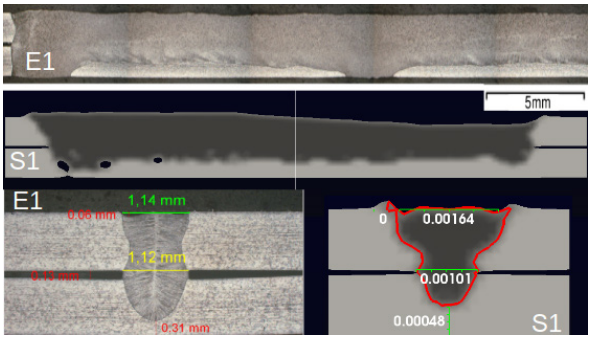

Fig. 2. Comparison between experiment E1 and simulation S1 (0.1mm gap).

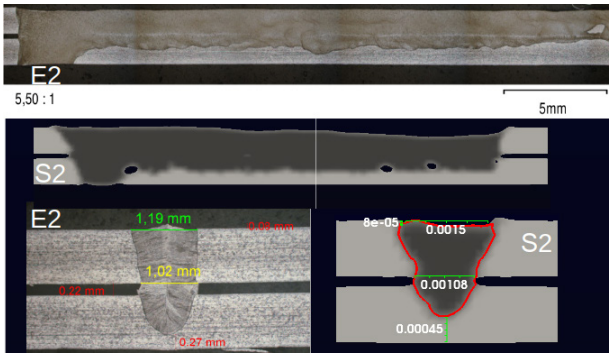

Fig. 3. Comparison between experiment E2 and simulation S2 (0.2 mm gap).

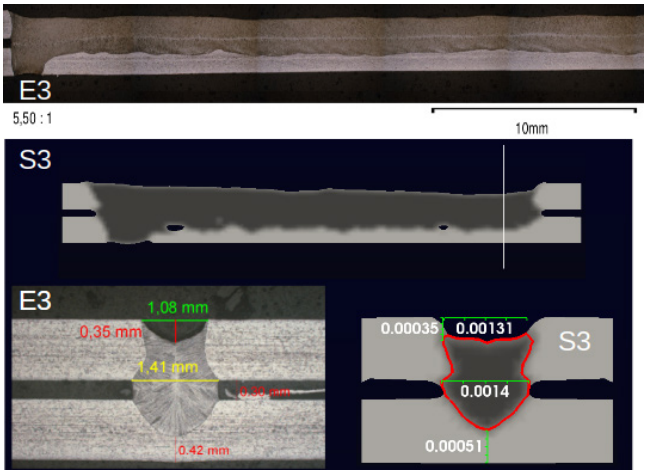

Fig. 4. Comparison between experiment E3 and simulation S3 (0.3 mm gap).

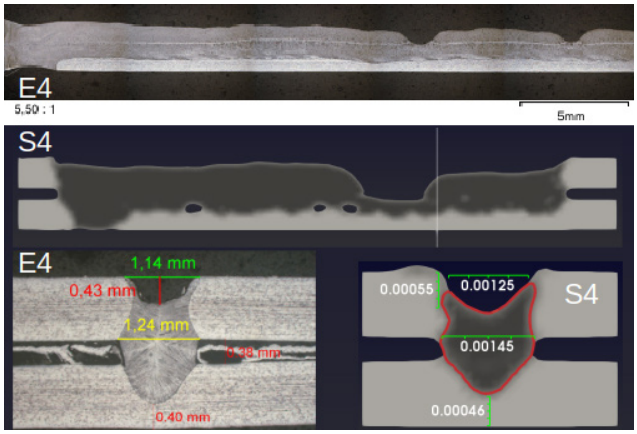

Fig. 5. Comparison between experiment E4 and simulation S4 (0.4 mm gap).

For the sake of simplicity, let us call the experiment green length “bead top width” and the yellow one “bead middle width”. Following Table 3 sums up the cross-section weld pool dimensions for experiments and simulation.

Table 3. Comparison between experimental and simulation weld pool cross-section dimensions

	bead top width (mm)		bead middle width (mm)		weld filling (mm)		penetration (mm)	
	val.	diff.	val.	diff.	val.	diff.	val.	diff.
E1	1.14	0.50	1.12	-0.11	0	0	-0.31	-0.17
S1	1.64		1.01		0		-0.48	
E2	1.1	0.31	1.02	0.06	+0.08	-0.08	-0.27	-0.18
S2	1.5		1.08		0		-0.45	
E3	1.08	0.23	1.41	-0.01	-0.35	0	-0.42	-0.09
S3	1.31		1.40		-0.35		-0.51	
E4	1.14	0.11	1.24	0.21	-0.43	-0.12	-0.40	-0.06
S4	1.25		1.45		-0.55		-0.46	

From Fig. 2, Fig. 3, Fig. 4 and Fig. 5, one can see that the longitudinal sections suit quite well the experiments. Simulations produce a few pores but the average behavior is comparable to experimental results. Surface shape and penetration seem consistent with the experiments. Even the surface defect from E4 is reproduced by S4.

S1 and S2 cross-sections do not quite suit the experimental ones, especially for the bead top width. Actually, one can also notice this behavior for, S3 and S4 but in a more reasonable extent. This issue certainly comes from a current model limitation on beam propagation, especially when M^2 gets higher. The bead middle width, however, seems to be in accordance with the experiments quite accurately.

In conclusion, both qualitatively and quantitatively, one can conclude that the model is well calibrated.

4. Defects analysis

4.1. Laser motion induced defect

A first noticeable defect or irregularity that one can see happens at the beginning of the process. The penetration goes from full to partial penetration. Actually, this defect is not

induced by the gap but by the laser motion. The simulation in Fig. 6 has been done based on S2 parameters but with an initial speed of 100 mm/s (no acceleration).

Fig. 6. Simulation based on S2 parameters and starting with a 100mm/s cruise speed (no acceleration).

One can see that a constant initial speed yields a constant penetration along the laser track.

4.2. Gap-induced defects

The first defect one can conclude from the presence of a gap is under-filling. The higher the gap is, the lower the re-solidified surface is. This phenomenon comes from a lack on material in the gap, the latter getting filled by the weld pool.

A second noticeable defect is the lack of penetration. From longitudinal and cross-sections, one can see that an increase in gap values induces a tendency to reduce penetration. A first explanation could be the beam divergence. Indeed, the higher the gap is, the longer the path is to reach the lower plate bottom and thus the wider is the waist radius. However, an increase of 0.1 mm in focus height induces an increase of approximately 4 µm in the beam waist. So this surely plays a role but a rather minor one. Another origin is an open keyhole. For high gap values, in S4 for instance, the keyhole opens in front of the laser (+Z direction). It thus induces less beam reflection and a lower heat absorption. One consequence is a lack of penetration.

The gap also has an influence on the bead middle width. From experimental cross sections, one can notice a value of 1.12 µm for E1 and 1.41 µm for E3. A first origin could be beam divergence, for the same reason as explained in the previous paragraph. The other reason is, let us call it, a “curtain” effect. The keyhole can be seen as a curtain (a kind of cylindrical curtain), attached between the upper and the lower plate. Laser induced vaporization in the keyhole exerts a radial force (in XZ plane) on this curtain. In +X, -X and +Z directions, there is no liquid or solid in the gap to resist to this over-pressure. The only counterbalancing force is a capillary one. However, this curtain still gets pushed radially. In +Z direction, the effects in front of the keyhole are erased by the next time steps. However, in +X and -X directions, this expansion tends to widen the heat affected zone and thus the re-solidified weld bead middle width.

Experiment E1 shows a stable weld process where a sudden instability (spike) reached the bottom plate and maintained full-penetration characteristics for a while (once the melt pool reaches the bottom, heat accumulation there helped to keep the full penetration). A longer simulation or even repeating the simulation by introducing any kind of surface imperfection in the middle of the path may allow for reproducing this effect.

Experiment E4 shows another type of instability. After approximately 2 cm, one can notice a wave-like re-solidified surface, around 1 mm deep. This phenomenon does not appear in E1, E2 or E3. From experimental results, it is hard to derive the origin for such a defect. The corresponding simulation S4 helps to understand the fluid dynamical failure mechanism. Fig. 7 (weld pool in dark grey). shows an interesting wave and explosion.

Fig. 7. Instability and explosion in simulation S4 between times t = 150ms and t = 152ms.

One can see in Fig. 7 that there is no connection between weld pool and upper plate at t = 150 ms. Suddenly, the weld pool reconnects with the upper plate ahead at t = 151 ms. This thin horizontal layer of reconnected weld pool, let us call it “bridge”, is being highly heated by the laser, then pushed by vapor expansion and seems to generate a wave leading to an instability and explosion in the rear weld pool.

Although that kind of instability might be out of the solver limit, one can still admit the unstable nature for a 0.4 mm gap.

5. Improvements on weld quality

5.1. Weld improvement through beam shaping

Unless adding welding material to the process, there is physically no way to substantially counterbalance under-fill with beam-shaping.

A way to investigate on penetration and bead middle width could be to play with the temperature distribution. Two different beam shapes called BS1 and BS2 are tested here. BS1 has almost the same set of parameters as for S1-4 but with a smaller spot waist on the surface: 92 µm. BS2 is the combination of an inner 1kW circular spot with a waist radius of 162 µm (on the surface) and an outer concentric 2.5kW circular spot with a waist radius of 226 µm (on the surface).

In order to avoid the re-connection instability leading to explosion seen in S4, a possibility is to diminish the fluence in Z-direction in order to create a less localized vapor expansion on the weld “bridge”. A simulation is done for a 3.5kW elliptical spot, with semi-major axis (in Z-direction) a = 339 µm and a semi-minor axis b = 226 µm. This beam shape is called BS3.

5.2. Beam shaping simulations results

The simulation for BS1 and BS2 are presented in Fig. 8 and Fig. 9. The latter respectively show the results obtained for longitudinal and cross sections.

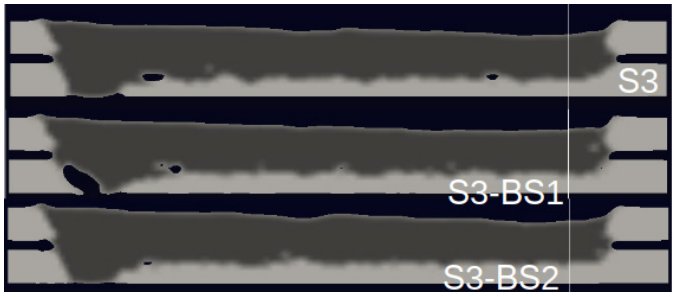

Fig. 8. Longitudinal sections of simulations S3 with from top to bottom: original parameters, BS1 and BS2.

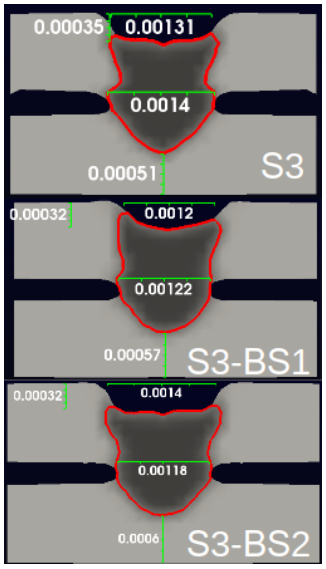

Fig. 9. Cross sections of simulations S3 with from top to bottom: original parameters, BS1 and BS2.

From Fig. 8 and Fig. 9, one can conclude that BS1 and BS2 do not provide a deeper penetration. Indeed, an easy way to get more penetration would be to slow down the laser speed, but this solution is out the paper scope. The bead middle width is smaller: 1.4 mm for S3, 1.22 mm for S3-BS1 and 1.18 mm for S3-BS2. S3-BS1 also yields a smaller bead top width (1.2 mm) and a more regular surface shape.

Fig. 10 (weld pool in dark grey) shows the results for a simulation based on S4 with a BS3 beam shape.

One can see that a weld bridge is built between time t = 149 ms and t = 150 ms. However, in opposition to the original S4 simulation, a lower concentrated heat input provides more stability and an explosion is avoided at t = 151 ms.

Fig. 10. Longitudinal section showing the stability of a weld bridge under an elliptical spot (parameters BS3) for a 0.4mm gap between times t = 0.149 ms and t = 0.151 ms.

Nevertheless, one has to remain careful using an elliptical spot and trying to stretch out the spot in the scanning direction. Fig. 11 shows the results obtained for a longer ellipse with semi-major and minor axis a = 452 µm and b = 226 µm respectively.

Fig. 11. Longitudinal section based on S4 parameters but with an elliptical spot (a = 452 µm and b = 226 µm on the surface) with semi-major axis in Z direction.

Indeed, a longer ellipse yields a less localized heat input which leads to a lack of penetration and thus to a lack of fusion between upper and lower plate.

6. Conclusion

The presence of a gap may induce particular welding defects, from under-fill, lack of penetration and too much wetting to instabilities and explosions in some cases. The presented simulations help to understand those defects and the gap influence on them.

A main defect being under-fill is hard to fully counterbalance through beam shaping and would require an additional weld material.

Two different techniques (smaller spot and two concentric beams) have been tried to influence penetration and bead middle width. Although the penetration decreased, a reduction of bead middle width and top width was noticeable.

The use of an elliptical spot has allowed for the control of an instability leading to an explosion in a 0.4 mm gap configuration.

The results presented here are still a work in progress and will be further tested through experiments. They should be taken as a tendency and an opening for further investigation on beam shaping solutions for gap induced welding defects.

7. Acknowledgements

This research work was funded by the European Commission within the Horizon 2020 project CUSTODIAN, which aims to develop a new dynamic beam shaping technology for optimizing Selective Laser Melting and Laser Welding processes.

8. References

[1] Otto, Andreas & Gomez Vazquez, Rodrigo & Hartel, Udo. (2018). Insight into the Process: Analysis of laser beam welding by means of multiphysical process simulations. Laser Technik Journal. 15. 40-45. 10.1002/latj.201800013.

[2] Lifang Mei, Genyu Chen, Dongbing Yan, Dan Xie, Xiaohong Ge, Mingjun Zhang, Impact of inter-sheet gaps on laser overlap welding performance for galvanised steel, Journal of Materials Processing Technology, Volume 226, 2015, Pages 157-168, ISSN 0924-0136, https://doi.org/10.1016/j.jmatprotec.2015.07.020.

[3] Cao, Xinjin & Debaecker, G. & Poirier, E. & Marya, Surendar & Cuddy, Jonathan & Birur, A. & Wanjara, P.. (2011). Tolerances of joint gaps in Nd : YAG laser welded Ti-6AI-4V alloy with the addition of filler wire. Journal of Laser Applications - J LASER APPL. 23. 10.2351/1.3554266.

[4] Koch, H., Gómez Vázquez, R., Otto, A., 2012. A Multiphysical Simulation Model for Laser Based Manufacturing. Proceedings of the 6th European Congress on Computational Methods in Applied Sciences and Engineering – ECCOMAS 2012, 4546.

[5] Otto, A., Koch, H., Gómez Vázquez, R., 2012. Multiphysical simulation of laser material processing. Proceedings of the 7th International Conference on Photonic Technologies LANE 2012. Physics Procedia 39, 843–852.

[6] Otto, A., Koch, H., Leitz K-H., Schmidt, M., 2011. Numerical Simulations - A Versatile Approach for Better Understanding Dynamics in Laser Material Processing. Proceedings of the Sixth International WLT Conference on Lasers in Manufacturing. Physics Procedia 12, Part A, 11–20.